RESEARCH ARTICLE | FEBRUARY 16 2017

# Optimization of the coplanar interdigital capacitive sensor



Yunzhi Huang; Zheng Zhan; Nicola Bowler



*AIP Conf. Proc.* 1806, 110017 (2017)
https://doi.org/10.1063/1.4974695



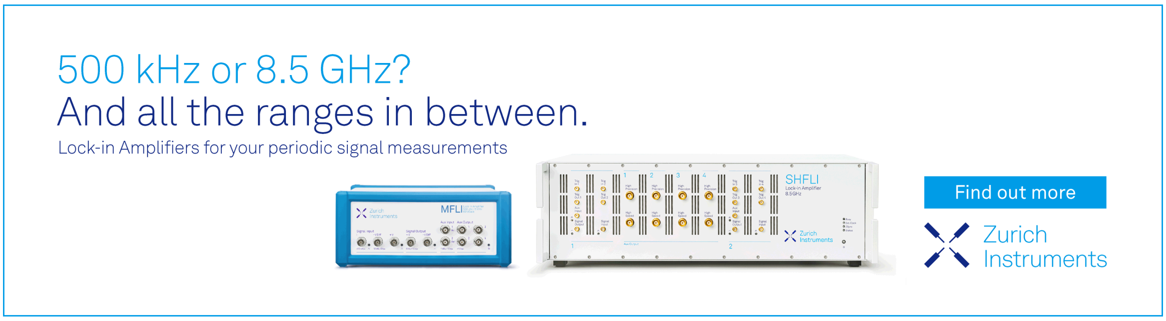

# Optimization of the Coplanar Interdigital Capacitive Sensor

Yunzhi Huang[1,2,a)], Zheng Zhan[1], and Nicola Bowler[2,3,b)]

[1] [1]*School of Electrical Engineering and Automation, Hefei University of Technology, Hefei, Anhui P.R. China*
[2]*Center for Non-destructive Evaluation, Iowa State University, Ames, IA, USA*
[3]*Departments of Materials Science and Engineering and of Electrical and Computer Engineering, Iowa State University, Ames, IA, USA*

[a)]hqyz@hfut.edu.cn
[b)]nbowler@iastate.edu

**Abstract.** Interdigital capacitive sensors are applied in nondestructive testing and material property characterization of low-conductivity materials. The sensor performance is typically described based on the penetration depth of the electric field into the sample material, the sensor signal strength and its sensitivity. These factors all depend on the geometry and material properties of the sensor and sample. In this paper, a detailed analysis is provided, through finite element simulations, of the ways in which the sensor's geometrical parameters affect its performance. The geometrical parameters include the number of digits forming the interdigital electrodes and the ratio of digit width to their separation. In addition, the influence of the presence or absence of a metal backplane on the sample is analyzed. Further, the effects of sensor substrate thickness and material on signal strength are studied. The results of the analysis show that it is necessary to take into account a trade-off between the desired sensitivity and penetration depth when designing the sensor. Parametric equations are presented to assist the sensor designer or nondestructive evaluation specialist in optimizing the design of a capacitive sensor.



## INTRODUCTION

Interdigital capacitive sensors are used widely for nondestructive measurement of dielectric material properties. One important advantage of such devices is that fringing electric fields associated with interdigital electrodes provide one-sided interrogation of the material-under-test. Active coatings applied to these devices allow detection of moisture, gases, and other substances [1-2]. The measurement of dielectric properties of insulating and semi-insulating materials also provides indirect information about their moisture content [3] and physical properties such as density [4], viscosity [5], porosity [6], and thickness [7]. By designing the electrodes such that the penetration depth can be varied, interdigital devices may in principle be used for three-dimensional imaging, but one difficulty in this regard is the non-uniform distribution of the fringing electric field, which is challenging to model.

In recent decades, interdigital capacitive sensors have been proposed for a diverse range of research and commercial applications. For example, an interdigital sensor has been applied for detecting insulation permittivity changes in aircraft wire as a function of its exposure to various fluids [8]. A quasi-electrostatic, semi-analytical model based on Green's function analysis and the Method of Moments was developed to calculate the capacitance of an interdigital sensor conformed to the curved surface of the wire insulation. Considering the effects of sensor geometry on its performance, results showed that there is a tradeoff between signal strength (measured capacitance) and sensing depth (extent of penetration of the electric field into the sample).

The design principles for interdigital concentric fringing electrical field sensors are presented in [9]. For imaging applications, the effect of sensor geometry on sensor performance is analyzed and the optimum balance of penetration depth and signal strength is proposed. In [10], a coplanar capacitive sensor is developed for detecting water intrusion into composite structures. A Maxwell 2D model is utilized to study the relationship between the capacitance across

*43rd Annual Review of Progress in Quantitative Nondestructive Evaluation, Volume 36*
AIP Conf. Proc. 1806, 110017-1–110017-9; doi: 10.1063/1.4974695
Published by AIP Publishing. 978-0-7354-1474-7/$30.00

the sensors and the geometrical parameters of the sensors. There is a trade-off between the signal strength and the field penetration depth. The optimal sensor parameters are achieved by proper selection of the electrode width and gap. A finite element simulation is employed to design a coplanar capacitive sensor in [11]. The sensor is applied to measure water content of building inclosure. The effects of the electrode width and electrode gap on the field strength are studied. The distance between adjacent electrode lines is assumed to be constant.

The performance of an interdigital capacitive sensor is typically assessed based on the penetration depth of its fringing field, its signal strength, and its sensitivity. All of these factors depend on the geometry and material properties of the sensor components and the sample. The primary goal of sensor design is to achieve the optimum balance among the desired performance characteristics. The sensor design task involves consideration of the desired sensitivity of the sensor, the necessary penetration depth of the sensor fields into the sample, and utilization of a rational approach to optimize the sensor geometry. This study describes the relationship between the sensor design parameters and its performance by utilizing a 3D finite element model (FEM). The sensor output capacitance is calculated as a function of the number of the electrode pairs, and of the ratio between the width and separation of the electrode digits. In addition, the influence of the presence or absence of a metal backplane on the sample is studied. Parametric equations are presented that express the sensor output capacitance and the penetration depth of its fringing electric field as functions of the sensor's geometrical parameters. The results enable sensor designers or nondestructive evaluation specialists to understand the relationships between the geometrical parameters and the characteristics of the interdigital capacitive sensor without repeating the time-consuming finite element simulations. The simulation results were validated through experimental testing of five capacitors with different geometrical parameters.

## SENSOR CONFIGURATION

The coplanar interdigital capacitive sensor is composed of driving electrodes, sensing electrodes, a dielectric substrate and a metal backplane. The electrodes are interdigitated. The periodicity $\lambda$ is defined as the distance between adjacent digits of the same polarity. The number of the electrode pairs is defined as $N$. A perspective view of the interdigital sensor is shown in Fig. 1(a) and a cross-sectional view in Fig. 1(b).



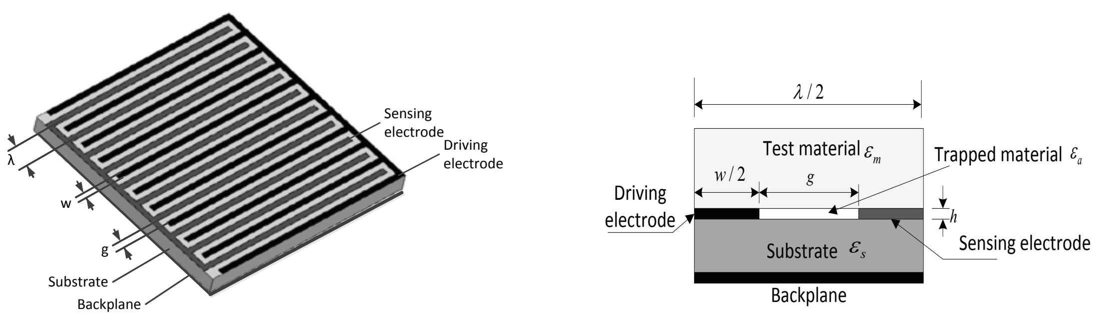


(a) (b)

**FIGURE 1.** Schematic views of the coplanar interdigital capacitive sensor; (a) Perspective view; (b) Cross-sectional view. $\varepsilon_m$, $\varepsilon_s$ and $\varepsilon_a$ are the relative permittivity of the test material, the sensor substrate and the material 'trapped' between the electrodes (usually air), respectively; *h* is the electrode thickness, *g* is the gap length between the electrodes, and *w* is the electrode width.

## SENSOR PERFORMANCE PARAMETERS

### Sensitivity

Sensitivity is defined as $s = \partial C / \partial \varepsilon$, the ratio between the variation in output capacitance and the variation in dielectric constant of the test material that gives rise to it. In cases where the capacitance is a linear function of the test-piece permittivity, $s$ is expressed as follows:

$$s = \frac{C_m - C_0}{\varepsilon_m - \varepsilon_0} \tag{1}$$

where $C_0$ is the value of sensor capacitance without the test material, $C_m$ represents the sensor capacitance when the sensor is in contact with an intermediate thickness of test material, $\varepsilon_m$ is the relative permittivity of the test-piece and the relative permittivity of air is $\varepsilon_0$. In other cases the sensitivity can be defined as the gradient of the change in measured capacitance as a function of test-piece permittivity. The greater the sensitivity, the bigger the variation of the output capacitance as a function of changes in the relative permittivity of the sample. High sensitivity is desirable so that changes in the dielectric properties of the test sample can be easily detected.

## Penetration Depth

The penetration depth P of coplanar interdigital capacitive sensors can be calculated as the depth at which the following expression holds [9]:

$$\frac{C_m - C_0}{C_{\max} - C_0} \times 100\% = 97\% \tag{2}$$

In (2), $C_0$ and $C_m$ are as defined above and $C_{\max}$ is the asymptotic (highest) value of sensor capacitance achieved for a particular test-material (in contact with the sensor electrodes) as its thickness is increased. Note that $C_m \rightarrow C_0$ as the thickness of the test-piece tends to zero.

# SENSOR DESIGN OPTIMIZATION

The width of the electrode digits and the gap size between them are two key factors affecting the sensor penetration depth. The sensor sensitivity and the signal strength increase slightly as the electrode thickness h increases but thicker electrodes generally waste electrical energy because the electric field lines traversing the gap provide no information useful for characterization of the sample. For this reason, the electrode thickness should be reduced as far as possible, limited only by the sensor processing technology. Likewise, it is beneficial to keep the dielectric constant of the sensor substrate as low as possible in order to increase the intensity of the fringing fields in the test-piece, but the sensor substrate is also designed based on the available processing technology and intended operating environment, including such considerations as necessary rigidity or flexibility of the sensor and expected temperature and humidity variations of the operating environment. Since the sensor's sensitivity and signal strength are proportional to the number of electrode digits and their length, we can also boost these by increasing N and the electrode length, where sample geometry allows.

In this section, the effects on sensor capacitance, sensitivity and field penetration depth are analyzed via FEM simulation as the sensor parameters N and $w/g$ are varied. The FEM model utilized is Maxwell 3D. Two cases are considered: i) air-backed dielectric sample and ii) metal-backed dielectric sample. The electric field distribution in the sensor substrate and in the samples is also presented in particular examples of these two cases.

## Air-backed Dielectric Sample

### *FEM Calculations*

Between the plates of a large, parallel-plate capacitive sensor filled with homogeneous dielectric material, the electric field is spatially uniform except near the capacitor edges. In contrast, the fringing electric field of the coplanar interdigital capacitive sensor is spatially non-uniform. The electric field distribution in the case of a particular sensor and dielectric sample is shown in Fig. 2.

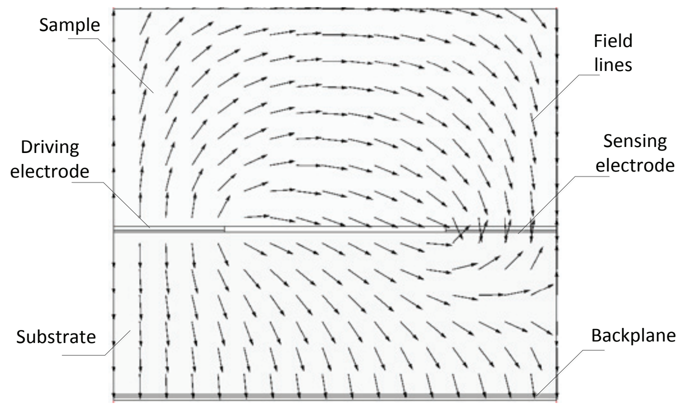


**FIGURE 2.** Electric field distribution in the vicinity of a coplanar interdigital capacitive sensor. The vector electric field is indicated by arrows. In this example, the sensor periodicity λ is 8 mm, the electrode thickness $h$ is 0.05 mm, the gap length $g$ and the finger width w are 2 mm, the substrate is 1.5 mm thick, has dielectric constant 4.4, and the sensor backplane is grounded. The thickness of the sample dielectric material is 2 mm with dielectric constant 4.5.

It is difficult to construct an analytical model for an interdigital capacitive sensor with finite overall dimensions because of its spatially non-uniform electrical field. In this study, a 3D FEM was utilized to evaluate the effects of sensor geometrical parameters on the output capacitance, the sensitivity, and the penetration depth. In the simulations, the sensor head area is constrained to be 20 × 20 mm2 , the substrate material is FR4 with dielectric constant 4.4 and assumed thickness 1.5 mm, the electrode thickness h and the backplane thickness are assumed to be 0.018 mm, and the test-piece is 2 mm with dielectric constant 4.5. Note, whereas FR4 is a readily available substrate material commonly used in electrical circuits, other substrate materials may be preferred for some applications. Teflon$^{TM}$, for example, is highly chemically stable, has dielectric constant of approximately 2.2, and is flexible when sufficiently thin.

The effect on the output capacitance of varying the ratio w/g and the number of electrode pairs, N, is shown in Fig. 3. As can be seen, the capacitance increases as the ratio w/g increases, and also as N increases.

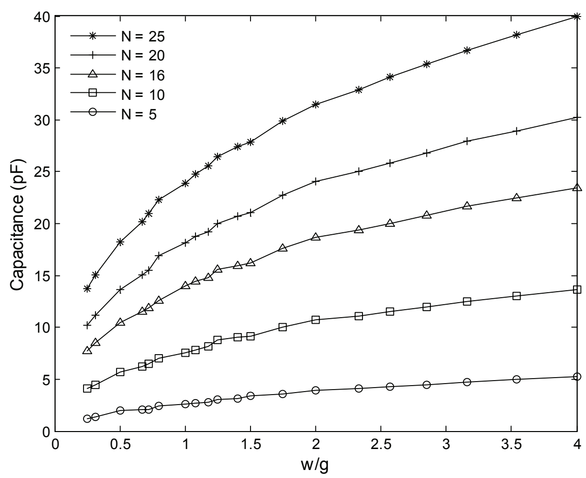


**FIGURE 3.** Calculated sensor capacitance as a function of the ratio $w/g$ and the number $N$, with no sample present. In the simulations, the sensor head area is constrained to be 20 × 20 $mm^2$ , the substrate is FR4 with dielectric constant 4.4 and assumed thickness 1.5 mm, the electrode thickness $h$ and the metal backplane thickness are both assumed to be 0.018 mm.

The sensitivity of the sensor, defined in (1), is studied by calculating the corresponding sensor capacitance as the parameters w/g and N are varied. In this calculation, the relative permittivity of the dielectric sample is assumed to be 5. Fig. 4 shows the effect of varying w/g and N on the sensor's sensitivity. It is seen that the sensitivity increases as the ratio w/g increases, and as N increases.

In addition to the sensitivity, the penetration depth, defined in (2), is also affected by changing the ratio w/g and the number of electrode pairs, N. Fig. 5 shows the effect on the penetration depth of changing w/g and N. As can be seen, the penetration depth decreases as the ratio w/g increases.

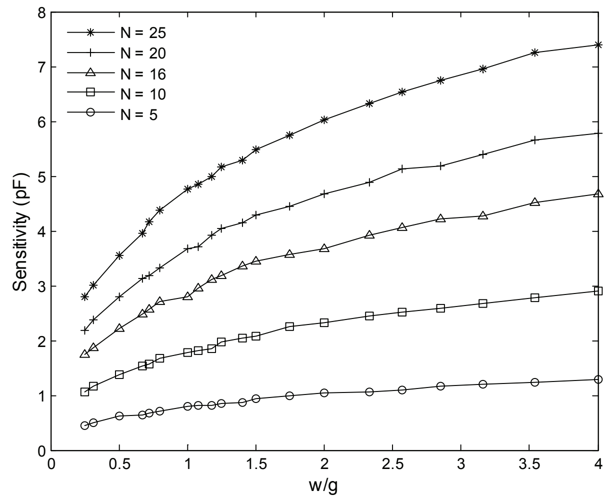


**FIGURE 4.** Capacitor sensitivity as a function of the ratio $w/g$ and $N$, for the same sensor described in Fig. 3 in contact with a test-piece with relative permittivity 4.5 and thickness 2 mm.

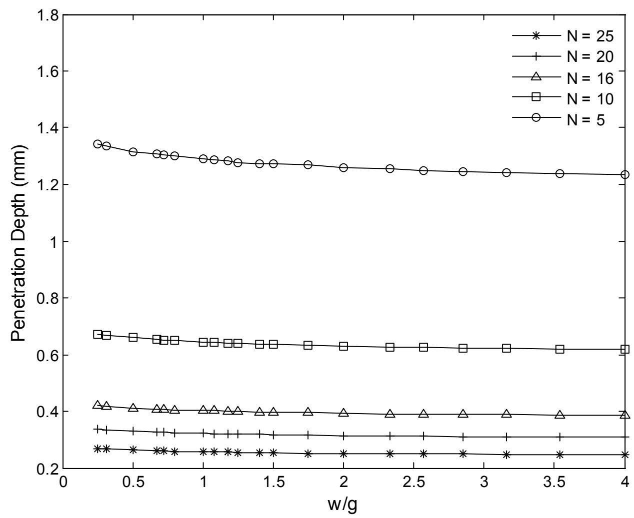


**FIGURE 5.** Penetration depth as a function of the ratio w/g and N. The sensor parameters are as for Fig. 3. The relative permittivity of the test-piece is 4.5 and its thickness is 2 mm.

### *Parametric Equations*

As can be inferred from Fig. 3, the capacitance as a function of the ratio w/g can be fitted with a second order polynomial,

$$\mathrm{C} = \varphi_0 + \varphi_1(w/g) + \varphi_2(w/g)^2 \tag{3}$$

wherein the coefficients $\varphi_i$ are linear functions of $N$ such that

$$\varphi_i = k_i N + b_i \, , i = 0, 1, 2 \tag{4}$$

and, inserting (4) into (3),

$$\mathrm{C} = \sum_{i=0}^{2} (k_i N + b_i)(w/g)^i \tag{5}$$

For a known substrate and test-piece, the coefficients $k_i$ and $b_i$ can be evaluated by fitting the curves shown in Fig. 3. In the case that the substrate is FR4 with dielectric constant 4.4 and assumed thickness 1.5 mm, with electrode and backplane thicknesses assumed to both be 0.018 mm, then the appropriate coefficients $k_i$ and $b_i$ are listed in Table 1.

**TABLE 1.** Coefficients in Eq. (5) obtained by fitting curves shown in Fig. 3 in the case when the substrate is FR4 with dielectric constant 4.4 and thickness 1.5 mm, and the electrode and backplane thicknesses are assumed to be 0.018 mm.

| $i$ | $k_i$ | $b_i$ |
|---|---|---|
| 0 | 0.5578 | 2.130 |
| 1 | 0.5424 | −0.7609 |
| 2 | −0.06632 | 0.1084 |

Considering the effects on penetration depth, the ratio $w/g$ and N play different roles. The function of the penetration depth and N is expressed as

$$P = \alpha_0 + \alpha_1 e^{-\alpha_2 N} \quad (6)$$

When the ratio $w/g$ is changed, the coefficients also change. If $w/g$ is assumed to be 0.25, for example, the penetration depth is

$$P = 0.26 + 2.739e^{(-0.186N)} \quad (7)$$

## Metal-backed Dielectric Sample

Metal coatings play an important role in industrial applications. Dielectric materials can be protected from friction, corrosion and chemicals using a metal coating in addition to their function as a ground plane or other electrical role. Here, the effect on measurements made by the coplanar interdigital capacitive sensor of a metal backplane on the sample material is studied.

The electric field distribution is changed when the metal backplane is present. Fig. 6 shows the presence of field lines between the driving electrode and the metal layer in addition to the field lines from the driving electrode to the sensing electrode. The total electric field intensity increases. The output capacitance is the sum of the capacitance between the driving and sensing electrode and the capacitance between the driving electrode and the metal layer.

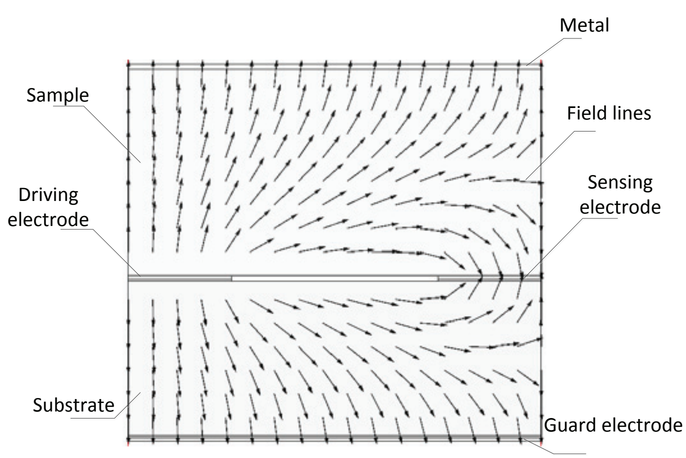


**FIGURE 6.** Electric field distribution in the vicinity of a coplanar interdigital capacitive sensor. Parameters are as for Fig. 2 but with a metal back-plane on the sample.

Considering the dielectric sample with metal-backing, the effect of the sample thickness on the output capacitance is studied. The effect of sample thickness is of particular interest in the case of the metal-backed samples because the electric field between the driving electrodes and the metal back-plane will change as the thickness increases. First, N is constrained to be 5, while the ratio $w/g$ is varied. Then, $w/g$ is constrained to be 1 and N is varied. As in the case of the air-backed dielectric sample, the sensor head area is constrained to be 20 × 20 mm2 , the substrate material is FR4 with dielectric constant 4.4 and assumed thickness 1.5 mm, the electrode thickness h and the backplane thickness are assumed to be 0.018 mm, and the test-piece permittivity is assumed to be 4.5. The results are shown in Fig. 7. The electric field between the driving electrode and the metal back-plane decreases as the sample thickness increases, giving rise to a corresponding decrease in the output capacitance. The output capacitance increases as the ratio $w/g$ increases and as N increases.

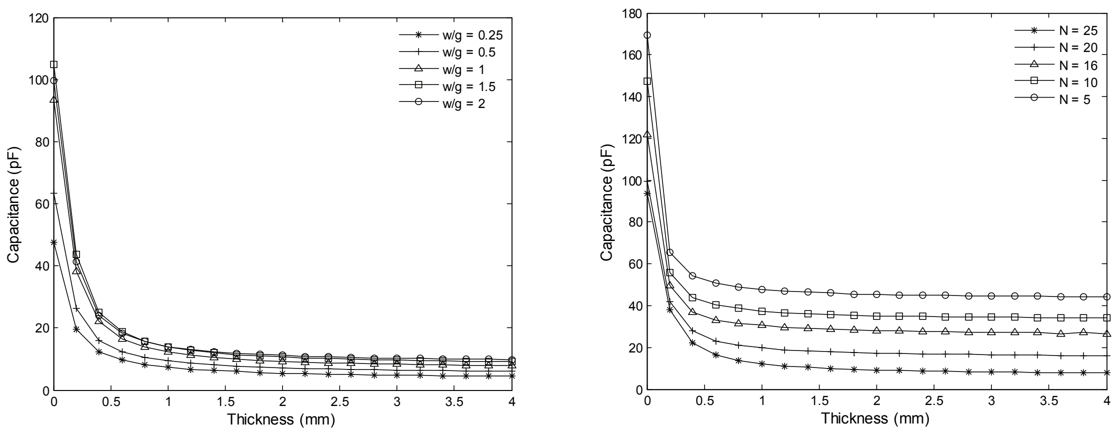


(a) (b)

**FIGURE 7.** The output capacitance versus the sample thickness. (a) $N$ is assumed to be 5; (b) $w/g$ is assumed to be 1. In the simulations, the sensor parameters are as for Fig. 3. The relative permittivity of test-pieces is 4.5.

The sensitivity is studied as described in section 4.1 and computed values in the case of a metal-backed dielectric sample are shown in Fig. 8. Comparing with sensitivity computed in the case of the dielectric sample without metal backing, Fig. 4, the value of the sensitivity computed here is much larger, increasing more rapidly as the ratio $w/g$ increases but increasing less rapidly as N increases.

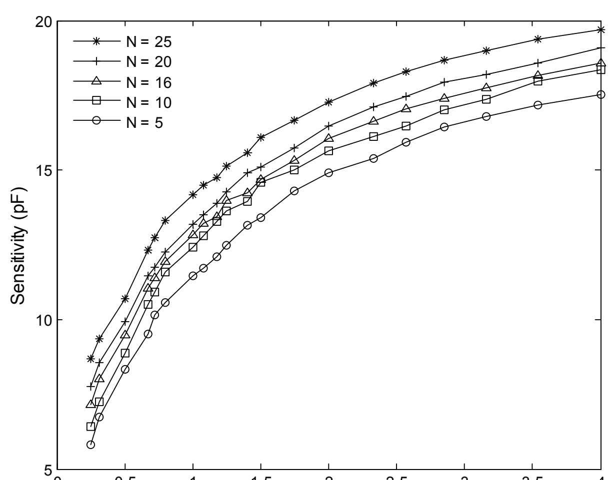


**FIGURE 8.** Sensitivity as the function of ratio $w/g$ and $N$ for a metal-backed dielectric sample. The sensor parameters are as for Fig. 3, for a sensor in contact with a test-piece with relative permittivity 4.5 and thickness 2 mm.

## EXPERIMENT

The design principles described in the previous section are illustrated and the calculations validated by experiments described in this section. Five sensor heads with different structure parameters $w/g$ and N were fabricated with printed-circuit-board technology, as shown in Fig. 9. The area of each sensor head was constrained to be approximately 20 × 20 $mm^2$.

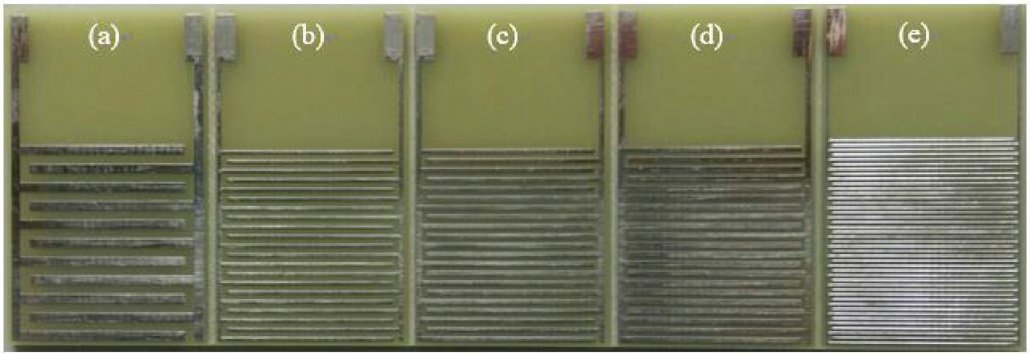


**FIGURE 9.** Capacitive sensor heads with different structure parameters: (a) $N = 5$, $w = g = 1$ mm; (b) $N = 10$, $w = 0.4$ mm, $g = 0.6$ mm; (c) $N = 10$, $w = g = 0.5$ mm; (d) $N = 10$, $w = 0.6$ mm, $g = 0.4$ mm; (e) $N = 20$, $w = g = 0.25$ mm. The substrate material is FR4 with thickness 1.5 mm and dielectric constant 4.4. The electrode thickness is 18 µm.

The type of dielectric sample is an air-backed Rogers RO3003 with thickness 0.506 mm. The repeatability error of the sensor is calibrated below 0.04 pF. The relative permittivity at 3.5 kHz is inferred from measured capacitance data for each of sensors (a) through (e), by utilizing the model, and the results are shown in Table 2. As a comparison, an Agilent E4980A Precision LCR Meter with Agilent 16451B test fixture (a parallel plate capacitor arrangement) were used to measure the permittivity of Rogers RO3003 at 3.5 kHz. The relative permittivity obtained is 2.880 ± 0.005. Comparing with the interdigital capacitive sensor measurement and the instrument measurement, the results illustrate that there is good agreement with relative difference below 4.5 % for the 10-digit sensors studied here. The relative difference is larger in the case of the five-digit and 20-digit sensors studied here due to the lower signal strength of the five-digit sensors and the lower penetration depth of the 20-digit sensor.



**TABLE 2.** Capacitance measured at 3.5 kHz using various sensor configurations of similar area, Fig. 10, with a Rogers RO3003 test piece, thickness 0.506 mm. Relative permittivity is inferred from Eq. (3) and compared with the value inferred from an independent measurement using traditional parallel plate electrodes with diameter 38 mm: 2.880 ± 0.005. Dimensions $w$ and $g$ are provided in the caption for Fig. 9.

| | **Sensor parameters** | | **Measured $C$ (pF)** | **Inferred relative permittivity** | **% uncertainty** | **% difference from directly-measured relative permittivity** |
|---|---|---|---|---|---|---|
| | $N$ | $w/g$ | | | | |
| (a) | 5 | 1 | 3.73 ± 0.02 | 2.73 ± 0.02 | 0.6 | 5.2 |
| (b) | 10 | 2/3 | 8.46 ± 0.03 | 2.79 ± 0.03 | 0.9 | 3.1 |
| (c) | 10 | 1 | 9.64 ± 0.02 | 2.77 ± 0.02 | 0.7 | 3.8 |
| (d) | 10 | 3/2 | 11.42 ± 0.03 | 2.75 ± 0.03 | 0.9 | 4.5 |
| (e) | 20 | 1 | 22.51 ± 0.02 | 2.68 ± 0.02 | 0.6 | 6.9 |

## CONCLUSION

This paper discusses the design parameters of an interdigital coplanar capacitive sensor and their role in successful non-destructive measurement of dielectric material properties of a test-piece with or without a metal back-plane. A three-dimensional finite element model was developed for the interdigital coplanar sensor. The effects of sensor geometry parameters on sensor performance were analyzed, in particular of the digit width-to-gap ratio, $w/g$, and the number of digits, N. It was shown that there is a design tradeoff between the sensor's sensitivity and the penetration depth of the fringing field into the test-piece. Parametric equations were presented, to assist the sensor designer or nondestructive evaluation specialist in optimizing the design of a capacitive sensor. A validation experiment showed that the sensor with optimized parameters gave the lowest relative difference between the value of the relative permittivity of an RO3003 dielectric sample measured with the interdigital sensor compared with that obtained from an independent parallel-plate capacitor measurement.

## ACKNOWLEDGEMENT

This work was financially supported by the China Scholarship Fund (No. 201406695031).

## REFERENCES

1. P.M. Faia, C.S. Furtado, and A.J. Ferreira. *Sensor Actuat. B-Chem.* **101**, 183 (2004).
2. S. Lei, C. Deng, Y. Chen, and Y. Li. *Sensor Actuat. A-Phys.* **167**, 231 (2011).
3. R.N. Dean, A.K. Rane, M.E. Baginski, J. Richard, Z. Hartzog, and D.J. Elton. *IEEE T. Instrum. Meas.* **61**, 1105 (2012).
4. S.M. Radke, and E.C. Alocilja. *Biosens. Bioelectron.* **20**, 1662 (2005).
5. R. Matsuzaki, S. Kobayashi, A. Todoroki, and Y. Mizutani. *Compos. Part A-Appl.* S. **42**, 782 (2011).
6. T.-T. Ngo, H. Shirzadfar, D. Kourtiche, and M. Nadi. *J. Nano-Electron. Phys.* **6**, 01001 (2014).
7. I. Matiss. *NDT&E International* **66**, 99 (2014).
8. R.T. Sheldon, and N. Bowler. *IEEE Sens. J.* **14**, 961 (2014).
9. X.B.B. Li, S.D. Larson, A.S. Zyuzin, and A.V. Mamishev. *IEEE Sens. J.* **6**, 434 (2006).
10. A.A. Nassr, W.H. Ahmed, and W.W.E. Dakhakhni. *Meas. Sci. Technol.* **19**, 1 (2008).
11. Z. Jun, X. Jingfeng, Y. Entao, Z. Keyin, and L. Haiqing. *Meas. Technol.* **01**, 7 (2008).